Current Biology 23, 2513–2518, December 16, 2013 ©2013 Elsevier Ltd All rights reserved http://dx.doi.org/10.1016/j.cub.2013.10.038

Report

Modeling Framework for the Establishment of the Apical-Basal Embryonic Axis in Plants

Krzysztof Wabnik,[1] Hélène S. Robert,[1,2] Richard S. Smith,[3,4] and Jiří Friml[1,2,5,*]

[1]Department of Plant Systems Biology, Flanders Institute for Biotechnology (VIB) and Department of Plant Biotechnology and Genetics, Ghent University, Technologiepark 927, 9052 Gent, Belgium

[2]Mendel Centre for Genomics and Proteomics of Plants Systems, Central European Institute of Technology (CEITEC), Masaryk University, 625 00 Brno, Czech Republic

[3]Institute of Plant Sciences, University of Bern, Altenbergrain 21, 3013 Bern, Switzerland

[4]Department of Comparative Development and Genetics, Max Planck Institute for Plant Breeding Research, Carl-von-Linné-Weg 10, 50829 Köln, Germany

[5]Institute of Science and Technology Austria, 3400 Klosterneuburg, Austria

Summary

The apical-basal axis of the early plant embryo determines the body plan of the adult organism. To establish a polarized embryonic axis, plants evolved a unique mechanism that involves directional, cell-to-cell transport of the growth regulator auxin. Auxin transport relies on PIN auxin transporters [1], whose polar subcellular localization determines the flow directionality. PIN-mediated auxin transport mediates the spatial and temporal activity of the auxin response machinery [2–7] that contributes to embryo patterning processes, including establishment of the apical (shoot) and basal (root) embryo poles [8]. However, little is known of upstream mechanisms guiding the (re)polarization of auxin fluxes during embryogenesis [9]. Here, we developed a model of plant embryogenesis that correctly generates emergent cell polarities and auxin-mediated sequential initiation of apical-basal axis of plant embryo. The model relies on two precisely localized auxin sources and a feedback between auxin and the polar, subcellular PIN transporter localization. Simulations reproduced PIN polarity and auxin distribution, as well as previously unknown polarization events during early embryogenesis. The spectrum of validated model predictions suggests that our model corresponds to a minimal mechanistic framework for initiation and orientation of the apical-basal axis to guide both embryonic and postembryonic plant development.

Results and Discussion

Concerted Feedback Loops Link Auxin Sources to Coordinated PIN Polarization

Data-driven computer models have been developed to study postembryonic plant patterning such as organogenesis, leaf patterning, or root development [10–17]. Despite that, no theoretical modeling framework for plant embryogenesis is available to date, thus limiting efforts to identify mechanisms for generating early polarization and patterning events in plants. We used an in silico approach to address potential mechanisms underlying the emergence of polarity and patterning during early embryogenesis. Our model integrates (1) a positive auxin feedback on PIN transcription mediated by TIR/AFB nuclear auxin receptors [4, 6, 18, 19] and (2) a negative effect on the internalization of PINs from the plasma membrane via extracellular auxin sensing [20] (Figure 1A). The extracellular perception might depend on the apoplastic pool of AUXIN BINDING PROTEIN 1 (ABP1) that is known to activate downstream ROP-based signaling [21, 22]. We have demonstrated that these concerted intra- and extracellular feedback loops [23] predict polarized canalization of auxin flow, e.g., during leaf vasculature patterning [24, 25].

To test the model behavior and robustness, we performed computer simulations on a single-cell layer representation (e.g., a line of cells) with initially uniform (nonpolar) PIN plasma membrane localizations (Figures 1C–1J). We varied model parameters and initial conditions such as the placement of the auxin source. If auxin production took place in the left-most cell of a cell file (Figure 1C, green arrow), asymmetric PIN localization, referred to as PIN polarity, was dynamically aligned toward the right-end of a cell file away from the auxin source (Figure 1C, blue arrow). This mirrors PIN polarity away from an auxin production typically observed during leaf venation patterning, shoot branching, or tissue regeneration processes [23, 26–29]. However, a contrasting output occurred when uniform auxin production with nonuniform (noisy) concentration fluctuations was introduced. PINs polarized toward cells with the highest auxin concentration (Figure 1D), similar to situation during organ initiation at the shoot apical meristem [30]. This PIN polarity toward auxin convergence maxima was further enhanced by saturating receptor occupancy resulting from high auxin levels in the apoplast that is shared by cells adjacent to these auxin maxima (Figure 1D). Furthermore, the predicted number of spontaneously generated, evenly spaced auxin peaks depended on number of simulated cells (Figures 1D–1F). This model was robust with respect to auxin degradation, auxin transport rates, and receptor dissociation rates (Figures 1G–1J; ±10-fold). However, the complete removal of the neighboring cell competition for extracellular auxin receptors yielded nonpolar PIN localizations (Figures 1A and 1J). Model parameters are described in Tables S2 and S3 (available online). Notably, this model could account for contrasting PIN polarization behavior toward and away from the auxin maxima using a single mechanism operating on different cellular auxin content that was so far missing in previous models [11, 13].

A Basal Auxin Source Is Sufficient to Polarize the Early Embryo for Apical Auxin Maximum

Next we tested whether our model (Figure 1A) predicts the polarization of auxin transport that underlie sequential establishment of apical and basal embryonic axis poles [8]. To perform simplified model simulations of early embryogenesis with the approximated complexity of cell growth by static embryo templates, we extracted embryos at the one-, two-,

*Correspondence: jiri.friml@ist.ac.at

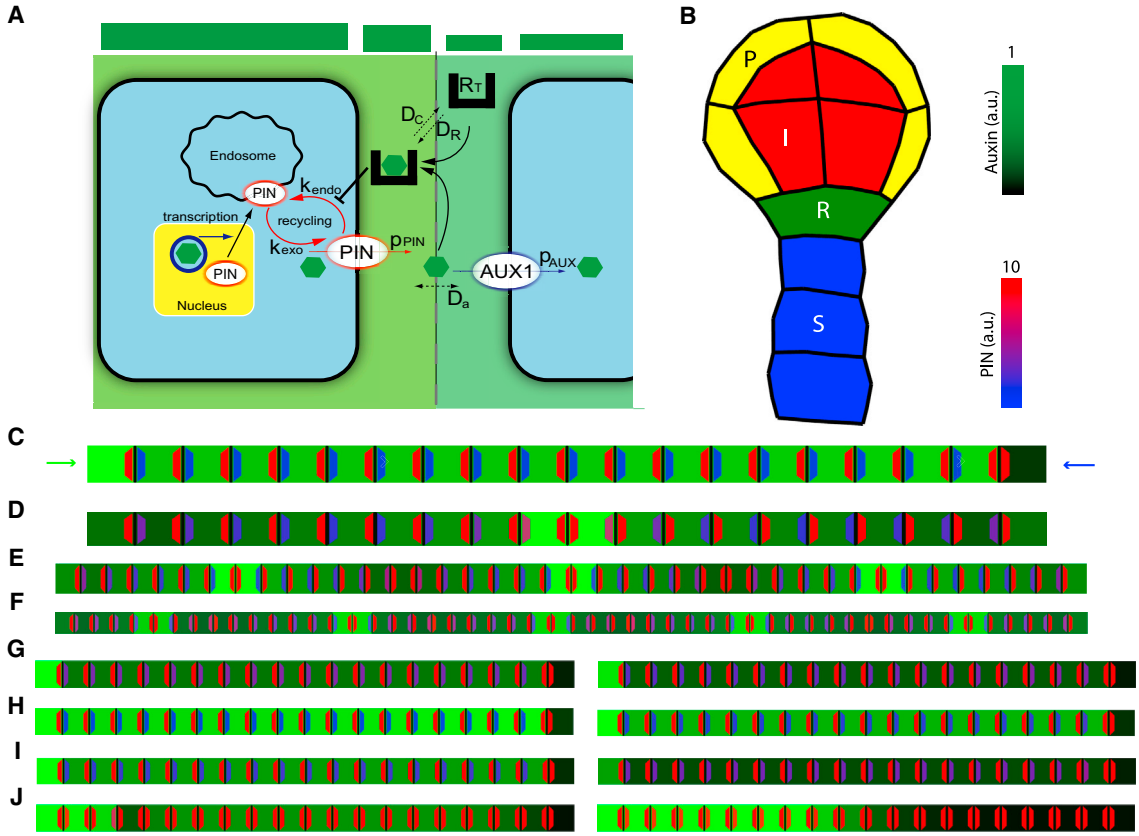

Figure 1. Model Schematics with Relevant Parameters and In Silico Analysis of Model Robustness

(A) Mechanistic framework for PIN subcellular dynamics regulated by auxin feedback mechanisms. Auxin (green hexagon) modulates the activity of PIN proteins by two independent feedback loops. PIN transcription is mediated by intracellular auxin signaling based on TIR1/AFBs auxin receptors (blue circle). PIN trafficking from the plasma membrane to endosomes (red arrows) is modulated by auxin perception through receptors in the cell wall (black open box). The effect of auxin-bound receptors on PIN internalization is enriched at the site of higher auxin concentration (green bars). Model parameters are described in Tables S2 and S3.

(B) Schematics of embryo template (16-cell stage) used in model simulations. The different cell types are marked with colors and letters: (S) blue, suspensor cells; (R) green, root pole; (I) red, inner proembryonic cells; and (P) yellow, protoderm cells. Color coding for auxin concentration (green) and PIN levels at the plasma membrane (blue for low PIN level and red for high PIN level) is shown. See also Figure S1.

(C) Canalization of auxin flows generated by the model simulated on cell file. Note the PIN polarity away from the source toward the sink. Green and blue arrows depict auxin source and auxin sink, respectively.

(D–F) Spontaneously generated, evenly spaced auxin maxima with a characteristic distance depending on cell number. Note that cells were polarized toward auxin peaks.

(G) Simulations with a 10-fold increase (value of 0.005 s^{-1}, left) and a 100-fold increase (value of 0.05 s^{-1}, right) of auxin degradation rate. Note that auxin production was set by default to 0.002 s^{-1}.

(H) A 10-fold decrease (left) and increase (right) in membrane permeabilities for PIN- and AUX-dependent auxin transport.

(I) Left: a 10-fold increase of receptor dissociation constant (value of 5 μM). Right: the parameter D_a was set to 5 $\mu m^2 s^{-1}$.

(J) Simulations of the model with no intercellular competition for auxin receptors (left). Parameters D_C and D_R were set to 1 $\mu m^2 s^{-1}$. Right: the parameter R_T was set to 0. Parameters are described in Tables S2 and S3.

See also Figures S1 and S2.

eight-, 16-, and 32-cell stages of their development from confocal microscopy images (Figures 1B and S1) using the MorphoGraphX software [31] (http://www.morphographx.org). We included the option to vary the location and strength of auxin-producing cells (auxin source) in the embryo model. Simulations of each developmental stage were initiated with a nonpolar PIN localization and uniform auxin concentrations.

When a hypothetical auxin source was positioned at the base of a one-cell embryo (consisting of a basal and an apical cell) to imitate an auxin inflow from the maternal tissues, the model predicted PIN polarity to the apical side of the basal cell pointing away from this basal source (green asterisk in Figure 2A; Movie S1), exactly as observed in planta for PIN7 protein [8]. No PIN polarity was predicted in the apical cell, whose apical cell membranes represent the embryo boundary with a no-flux condition. In accordance, so far no experimental data show a polar PIN localization in one-cell embryo. Thus, only PIN7-dependent auxin transport occurs in the basal cell of the one-cell embryos generating auxin accumulation in the apical cell both in in planta [8] and in the simulations (Figure 2A). These model predictions were robust over a wide range of biologically feasible parameter values (Figure S2A–S2M; ±10-fold). Similarly, apical PIN7-like polarity in the suspensor (derived from the basal cell) directed auxin to the proembryo (derived from the apical cell) in simulations of one-cell and eight-cell embryos (Figures 2B and 2C; Movies S2 and S3). Additionally, the model correctly predicted

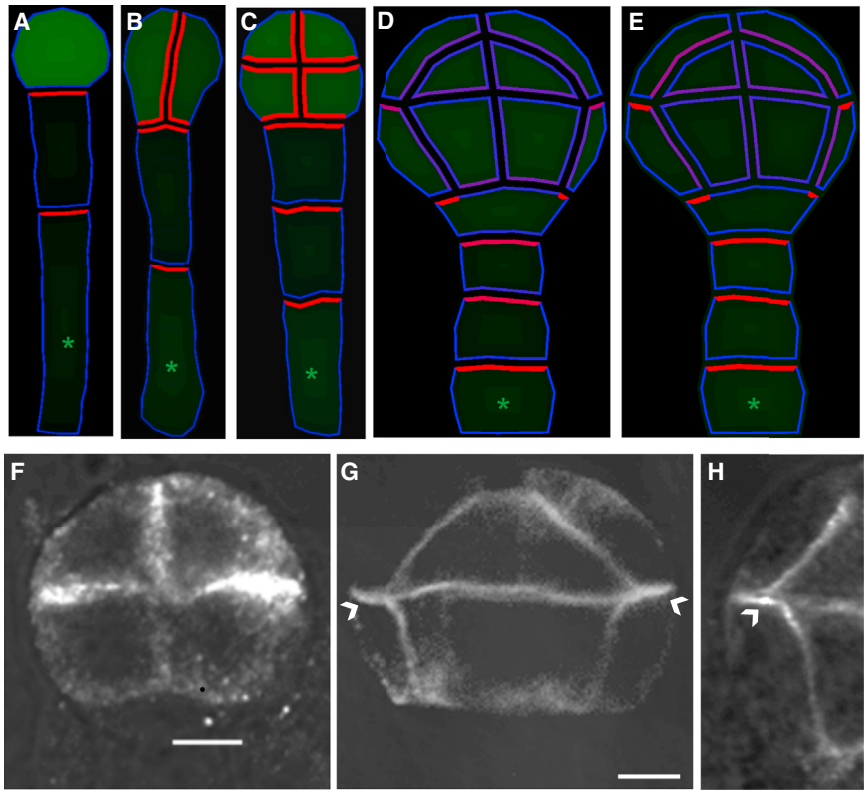

Figure 2. Computer Model Simulations with a Basal Auxin Source Predicting PIN Polarity and Auxin Accumulation

(A) The one-cell embryo model predicts PIN7-like polarization of the basal cell and moderate auxin accumulation in the apical cell. Auxin source (green asterisk) mimics auxin synthesis in the basal cell or supply from the maternal tissue (Movie S1).

(B and C) Two-cell and eight-cell embryo simulations demonstrate PIN polarization toward the embryo apex, local auxin accumulation, and preferentially nonpolar PIN localization in the proembryo (Movie S2).

(D and E) Computer model simulations of the 16-cell embryo with auxin production in the lowermost cell (green asterisk) predict PIN7 polarity in the suspensor and PIN1 polarity in the protoderm (D), but not the basal PIN1 polarity switch in inner proembryonic cells (E).

(F) PIN1 immunolocalization in eight-cell embryos. Apolar PIN1 localizations are shown.

(G and H) PIN1 immunolocalization in a 16-cell embryo showed that PIN1 polarity (white arrowheads) in the protoderm (H) occurred prior to its polarity in the inner cells (16%, n = 106, G).

Color coding for auxin concentration and PIN levels at the plasma membrane is as in Figure 1B. Scale bars represent 10 μm.

See also Figures S1 and S2 and Movies S1, S2, S3 and S4.

a ubiquitous and nonpolar PIN1 distribution in the two-cell and eight-cell proembryo (Figures 2C and 2F) [8]. These simulations on the earliest stages of embryogenesis showed that a basal auxin source coupled to feedback regulation of PIN polarities faithfully predicts auxin fluxes away from the maternal tissue toward the future embryo apex and auxin accumulation there.

Simulations with a Basal Auxin Source Predict Early PIN Polarity in Protoderm Cells

Next, we simulated the embryo model on a realistic 16-cell-stage embryo template (Figures 2D and 2E). Simulations predicted persistence of PIN7-like polarity in the suspensor toward the proembryo (Figure 2D). Notably, the model predicted emergent PIN1-like polarity of outer proembryo cells (protoderm) toward the proembryo apex (Figure 2D). This previously unappreciated PIN1 polarization resulted from a rapid PIN-dependent auxin inflow constrained by proembryo boundaries and would represent the earliest polarization event in proembryo preceding the known PIN1 basal polarity in the inner proembryo cells at the globular stage [8]. To test this prediction in planta, we performed PIN1 immunolocalization visualizing PIN1 at apical membranes of protoderm cells at 16-cell stage (Figures 2G and 2H, white arrowheads). Apolar PIN1 in both protoderm and inner cells was rarely observed (one out of 106 16-cell embryos). Notably, we regularly observed polar PIN1 in both protoderm and inner cells (88/106) and polar PIN1 in the protoderm but apolar in inner cells (17/106). However, we never observed the opposite situation with a polar PIN1 localization in the inner cells and apolar in protoderm (Figure 2G; Table S1). Thus, our feedback-based model with a basal auxin source predicted PIN polarity in the suspensor and the protoderm of early embryo stages. However, these model simulations integrating a single auxin source did not generate the subsequent PIN1-like localization to the basal membranes of the inner proembryonic cells (Figure 2E; Movie S4).

An Additional Apical Auxin Source Is Required for Auxin Transport Switch and Establishment of the Basal Auxin Maximum

Experimental observations showed that in young globular proembryos, PIN1 polarizes to the basal membranes of inner cells, an event preceding and being required for specification of the future root pole at the basal end of embryonic axis [8]. Hypothetically, an additional auxin source, located at the proembryo apex, could reverse auxin flow in the proembryo by generating a switch in PIN polarity. To test this hypothesis, we simulated a second source placed at the uppermost cells of the proembryo in the 16-cell embryo after initial protoderm PIN polarity had occurred (Figure 3A). The introduction of a second auxin source (Figure 3B) at this unique embryonic position sufficed for PIN1-like basal polarity in the inner cells. Consequently, the model predicted a downward auxin flow and auxin accumulation at the root pole (Figure 3B; Movie S5) and basal repolarization of PINs in suspensor cells (Figure 3B). Predicted PIN polarities were maintained in the simulations of 32-cell embryos (Figure 2C; Movie S6) regardless of the particular choices of model parameters, artificial geometry of embryo templates, or cell volumetric ratios (Figures S2I–S2S). Moreover, simulations of mutants with impaired auxin transport (Figures S2J and S2U), with no extracellular auxin perception (Figure S2T), and with randomly placed auxin sources (Figure S2V) displayed aberrant PIN polarities and auxin distribution patterns, indicating that embryo patterning largely depend on these processes [8, 32, 33]. Notably, the

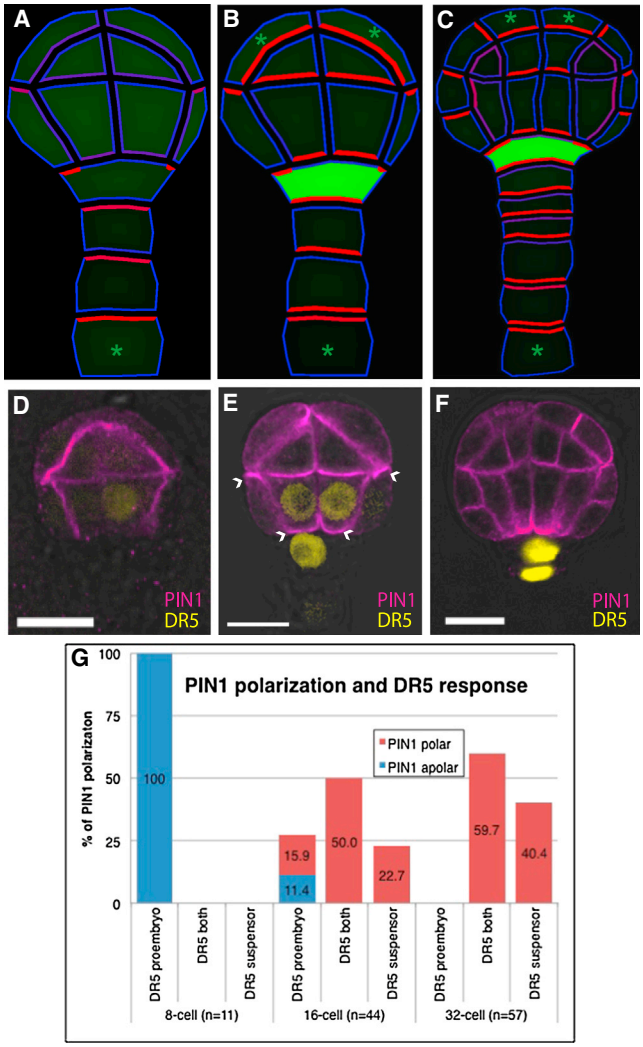

Figure 3. Computer Model Simulations with Sequential Basal and Apical Auxin Sources Predicting PIN Polarity and Auxin Accumulation

(A and B) Simulations of a 16-cell embryo model with the sequential introduction of auxin production (green asterisks), initially at the base of the suspensor (A) and later in the two most apical cells (B, Movie S4).

(C) PIN polarity and auxin distribution patterns were maintained in a 32-cell embryo (Movie S5).

(D–F) PIN1 (magenta) immunolocalization in *DR5::N7-Venus* (yellow) embryos. Apolar PIN1 in inner cells and DR5 maximum in proembryo at 16-cell stage (D, n = 106; see also Figure 2H). Most embryos displayed polarized PIN1 in protoderm and inner cells correlating with gradual DR5 shift to the root pole (E, white arrowheads). A globular embryo with polarized PIN1 and root pole DR5 maximum is shown in (F). Scale bars represent 10 μm.

(G) Correlated PIN1 polarity with the auxin response pattern (DR5 reporter). Numbers and bars represent a percentage of embryos showing either absence (blue) or presence (red) of PIN1 on basal membranes of inner cells versus the DR5 response pattern. n represents the number of analyzed embryos.

See also Figures S1 and S2, Table S1, and Movies S5 and S6.

assumption of a less effective PIN7-mediated auxin transport from the auxin maximum as compared to PIN1-mediated supply to this cell from the proembryo as derived from different "transporting surfaces" [8] was necessary to predict well-defined auxin maxima at root pole but not PIN polarities (Figure S2W).

Experimental Validations of Model Predictions for PIN Polarity and Auxin Maxima

To validate model predictions, we examined the correlation of PIN1 polarity in inner embryonic cells with the activity of auxin response reporter *DR5:N7-Venus* [34] during embryogenesis. In 16-cell embryos, apolar PIN1 in the inner cells (note the stronger PIN1 signal at more-recent cell boundaries between inner cells and protoderm) is concomitant with a weak auxin response maximum exclusively in the proembryo (11% of 16-cell embryos, n = 44; Figures 3D and 3G; Table S1). At the same developmental stage, PIN1 progressively localized to the basal membranes of the inner cells facing the future root pole (72% of 16-cell embryos, n = 44; Figure 3E). This PIN1 polarization preceded the shift of the DR5 auxin response maximum to the root pole (Figures 3F and 3G; Table S1). These observations show that PIN1 polarization toward the embryo base occurs at a sharply defined moment at the 16-cell stage and immediately precedes the establishment of the basal auxin maximum, fully agreeing with model predictions. The central importance of the secondary auxin source in the proembryo was further experimentally validated by the accompanying study [35], demonstrating that its absence leads to severe defects in PIN1 polarity and in basal auxin maximum formation, exactly as predicted by the model (Figure 2E).

Conclusions

We propose a model of the plant embryo that generates an experimentally verified pattern of cell polarities and sequential auxin response maxima from an apolar starting situation. Model simulations indicate that a basal auxin source at the one-cell stage (for example, provided by maternal tissues) is sufficient to trigger polarity of PIN7 auxin transporters toward the apical cell where auxin accumulation and downstream responses mediate the specification of the apical pole of the embryonic axis, the proembryo (Figure 4A). As the proembryo develops, protoderm cells display PIN1 polarity toward the proembryo apex, where a second auxin source arises (Figure 4B). This secondary source triggers PIN1 polarity in the inner embryonic cells and directs auxin to the basal pole for root specification (Figure 4C). The close agreement between the model predictions and experimental observations [8, 35] suggests that a coordinated local auxin production occurring at opposite ends of the plant embryo and feedback mechanisms suffices for orienting the embryonic axis for auxin-guided patterning of basal and apical embryo poles.

Intra- and intercellular feedback loops at the core of our model are realized by biologically traceable molecular components such as the TIR1/AFB nuclear auxin receptor [4, 6] and the ABP1 putative extracellular auxin receptor [20, 33] acting upstream of the associated ROP-GTPase-dependent signaling pathway [21, 22]. We believe that this embryo modeling framework can be further extended to address other molecular components and mechanisms acting in concert or parallel with auxin flux-based mechanisms, such as the involvement of mobile transcription factors in radial patterning [36] or root pole specification [37]. The presented model can be easily adapted for analogical situations of new growth axes specification and tissue polarization during later stages of embryonic or postembryonic development, such as de novo organogenesis, thus providing a valuable tool to test various hypotheses related to different aspects of plant development.

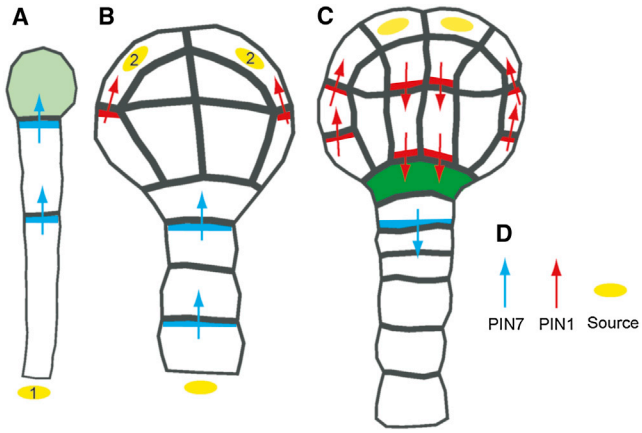

Figure 4. Modeling Framework for Early Embryo Patterning

(A) The one-cell embryo receives auxin from maternal tissues (1) that polarizes PIN7 auxin transporters to the apical side of the suspensor cells (magenta arrows). PIN7-dependent auxin accumulation in the future proembryo is shown.

(B) The 16-cell embryo initially displays PIN1 polarity to the apical side of protoderm cells (red bars) that determines the auxin flux through embryo boundaries. This polarization event coincides with initiation of autonomous auxin production in the proembryo uppermost cells (2).

(C) At the globular (16- or 32-cell) stage of embryogenesis, autonomous auxin production in the proembryo results in a auxin transport switch, manifested by basal PIN1 and PIN7 (red and blue bars) polarity and subsequent transport-dependent auxin accumulation in the uppermost suspensor cell marking the future root pole. Arrows show a preferential direction of auxin transport.

(D) Legend for symbols used in (A)–(C).

Supplemental Information

Supplemental Information includes Supplemental Experimental Procedures, two figures, three tables, and six movies and can be found with this article online at http://dx.doi.org/10.1016/j.cub.2013.10.038.

Author Contributions

K.W., H.S.R., and J.F. planned experiments. K.W., H.S.R., and R.S. performed experiments. K.W., H.S.R., and J.F. analyzed the data. K.W., H.S.R., and J.F. wrote the paper.

Acknowledgments

We thank N. Smet for plant care, J. Kleine-Vehn for discussion and comments and E.M. Meyerowitz for providing seeds. This work was supported by grants from the European Social Fund (CZ.1.07/2.3.00/20.0043), the European Research Council (project ERC-2011-StG-20101109-PSDP) and project "CEITEC - Central European Institute of Technology" (CZ.1.05/1.1.00/02.0068) to J.F. and from a Swiss National Science Foundation SystemsX.ch grant to R.S.S. H.S.R acknowledges a support from the Employment of Best Young Scientists for International Cooperation Empowerment (CZ.1.07/2.3.00/30.0037), cofinanced by the European Social Fund and the state budget of the Czech Republic.

Received: April 19, 2013
Revised: September 17, 2013
Accepted: October 15, 2013
Published: November 27, 2013

References

1. Petrásek, J., Mravec, J., Bouchard, R., Blakeslee, J.J., Abas, M., Seifertová, D., Wisniewska, J., Tadele, Z., Kubes, M., Covanová, M., et al. (2006). PIN proteins perform a rate-limiting function in cellular auxin efflux. Science *312*, 914–918.
2. Smith, Z.R., and Long, J.A. (2010). Control of Arabidopsis apical-basal embryo polarity by antagonistic transcription factors. Nature *464*, 423–426.
3. Ueda, M., Zhang, Z., and Laux, T. (2011). Transcriptional activation of Arabidopsis axis patterning genes WOX8/9 links zygote polarity to embryo development. Dev. Cell *20*, 264–270.
4. Vernoux, T., Brunoud, G., Farcot, E., Morin, V., Van den Daele, H., Legrand, J., Oliva, M., Das, P., Larrieu, A., Wells, D., et al. (2011). The auxin signalling network translates dynamic input into robust patterning at the shoot apex. Mol. Syst. Biol. *7*, 508.
5. Brunoud, G., Wells, D.M., Oliva, M., Larrieu, A., Mirabet, V., Burrow, A.H., Beeckman, T., Kepinski, S., Traas, J., Bennett, M.J., and Vernoux, T. (2012). A novel sensor to map auxin response and distribution at high spatio-temporal resolution. Nature *482*, 103–106.
6. Chapman, E.J., and Estelle, M. (2009). Mechanism of auxin-regulated gene expression in plants. Annu. Rev. Genet. *43*, 265–285.
7. Rademacher, E.H., Lokerse, A.S., Schlereth, A., Llavata-Peris, C.I., Bayer, M., Kientz, M., Freire Rios, A., Borst, J.W., Lukowitz, W., Jürgens, G., and Weijers, D. (2012). Different auxin response machineries control distinct cell fates in the early plant embryo. Dev. Cell *22*, 211–222.
8. Friml, J., Vieten, A., Sauer, M., Weijers, D., Schwarz, H., Hamann, T., Offringa, R., and Jürgens, G. (2003). Efflux-dependent auxin gradients establish the apical-basal axis of Arabidopsis. Nature *426*, 147–153.
9. Kepinski, S., and Leyser, O. (2003). Plant development: an axis of auxin. Nature *426*, 132–135.
10. Smith, R.S. (2008). The role of auxin transport in plant patterning mechanisms. PLoS Biol. *6*, e323.
11. Prusinkiewicz, P., and Runions, A. (2012). Computational models of plant development and form. New Phytol. *193*, 549–569.
12. Roeder, A.H., Tarr, P.T., Tobin, C., Zhang, X., Chickarmane, V., Cunha, A., and Meyerowitz, E.M. (2011). Computational morphodynamics of plants: integrating development over space and time. Nat. Rev. Mol. Cell Biol. *12*, 265–273.
13. Jönsson, H., Gruel, J., Krupinski, P., and Troein, C. (2012). On evaluating models in computational morphodynamics. Curr. Opin. Plant Biol. *15*, 103–110.
14. Grieneisen, V.A., Xu, J., Marée, A.F., Hogeweg, P., and Scheres, B. (2007). Auxin transport is sufficient to generate a maximum and gradient guiding root growth. Nature *449*, 1008–1013.
15. Walker, M.L., Farcot, E., Traas, J., and Godin, C. (2013). The flux-based PIN allocation mechanism can generate either canalyzed or diffuse distribution patterns depending on geometry and boundary conditions. PLoS ONE *8*, e54802.
16. Kramer, E.M. (2009). Auxin-regulated cell polarity: an inside job? Trends Plant Sci. *14*, 242–247.
17. Swarup, R., Kramer, E.M., Perry, P., Knox, K., Leyser, H.M., Haseloff, J., Beemster, G.T., Bhalerao, R., and Bennett, M.J. (2005). Root gravitropism requires lateral root cap and epidermal cells for transport and response to a mobile auxin signal. Nat. Cell Biol. *7*, 1057–1065.
18. Vieten, A., Vanneste, S., Wisniewska, J., Benková, E., Benjamins, R., Beeckman, T., Luschnig, C., and Friml, J. (2005). Functional redundancy of PIN proteins is accompanied by auxin-dependent cross-regulation of PIN expression. Development *132*, 4521–4531.
19. Peer, W.A., Bandyopadhyay, A., Blakeslee, J.J., Makam, S.N., Chen, R.J., Masson, P.H., and Murphy, A.S. (2004). Variation in expression and protein localization of the PIN family of auxin efflux facilitator proteins in flavonoid mutants with altered auxin transport in Arabidopsis thaliana. Plant Cell *16*, 1898–1911.
20. Robert, S., Kleine-Vehn, J., Barbez, E., Sauer, M., Paciorek, T., Baster, P., Vanneste, S., Zhang, J., Simon, S., Čovanová, M., et al. (2010). ABP1 mediates auxin inhibition of clathrin-dependent endocytosis in Arabidopsis. Cell *143*, 111–121.
21. Chen, X., Naramoto, S., Robert, S., Tejos, R., Löfke, C., Lin, D., Yang, Z., and Friml, J. (2012). ABP1 and ROP6 GTPase signaling regulate clathrin-mediated endocytosis in Arabidopsis roots. Curr. Biol. *22*, 1326–1332.
22. Xu, T., Wen, M., Nagawa, S., Fu, Y., Chen, J.G., Wu, M.J., Perrot-Rechenmann, C., Friml, J., Jones, A.M., and Yang, Z. (2010). Cell surface- and rho GTPase-based auxin signaling controls cellular interdigitation in Arabidopsis. Cell *143*, 99–110.
23. Wabnik, K., Kleine-Vehn, J., Balla, J., Sauer, M., Naramoto, S., Reinöhl, V., Merks, R.M.H., Govaerts, W., and Friml, J. (2010). Emergence of tissue polarization from synergy of intracellular and extracellular auxin signaling. Mol. Syst. Biol. *6*, 447.

24. Sachs, T. (1981). The control of the patterned differentiation of vascular tissues. Adv. Bot. Res. *9*, 151–262.
25. Berleth, T., and Sachs, T. (2001). Plant morphogenesis: long-distance coordination and local patterning. Curr. Opin. Plant Biol. *4*, 57–62.
26. Sauer, M., Balla, J., Luschnig, C., Wisniewska, J., Reinöhl, V., Friml, J., and Benková, E. (2006). Canalization of auxin flow by Aux/IAA-ARF-dependent feedback regulation of PIN polarity. Genes Dev. *20*, 2902–2911.
27. Sawchuk, M.G., Edgar, A., and Scarpella, E. (2013). Patterning of leaf vein networks by convergent auxin transport pathways. PLoS Genet. *9*, e1003294.
28. Scarpella, E., Marcos, D., Friml, J., and Berleth, T. (2006). Control of leaf vascular patterning by polar auxin transport. Genes Dev. *20*, 1015–1027.
29. Prusinkiewicz, P., Crawford, S., Smith, R.S., Ljung, K., Bennett, T., Ongaro, V., and Leyser, O. (2009). Control of bud activation by an auxin transport switch. Proc. Natl. Acad. Sci. USA *106*, 17431–17436.
30. Bayer, E.M., Smith, R.S., Mandel, T., Nakayama, N., Sauer, M., Prusinkiewicz, P., and Kuhlemeier, C. (2009). Integration of transport-based models for phyllotaxis and midvein formation. Genes Dev. *23*, 373–384.
31. Kierzkowski, D., Nakayama, N., Routier-Kierzkowska, A.L., Weber, A., Bayer, E., Schorderet, M., Reinhardt, D., Kuhlemeier, C., and Smith, R.S. (2012). Elastic domains regulate growth and organogenesis in the plant shoot apical meristem. Science *335*, 1096–1099.
32. Friml, J., Benková, E., Blilou, I., Wisniewska, J., Hamann, T., Ljung, K., Woody, S., Sandberg, G., Scheres, B., Jürgens, G., and Palme, K. (2002). AtPIN4 mediates sink-driven auxin gradients and root patterning in Arabidopsis. Cell *108*, 661–673.
33. Chen, J.G., Ullah, H., Young, J.C., Sussman, M.R., and Jones, A.M. (2001). ABP1 is required for organized cell elongation and division in Arabidopsis embryogenesis. Genes Dev. *15*, 902–911.
34. Weijers, D., Schlereth, A., Ehrismann, J.S., Schwank, G., Kientz, M., and Jürgens, G. (2006). Auxin triggers transient local signaling for cell specification in Arabidopsis embryogenesis. Dev. Cell *10*, 265–270.
35. Robert, H.S., Grones, P., Stepanova, A.N., Robles, L.M., Lokerse, A.S., Alonso, J.M., Weijers, D., and Friml, J. (2013). Local auxin sources orient the apical-basal axis in *Arabidopsis* embryos. Curr. Biol. Published online November 27, 2013. http://dx.doi.org/10.1016/j.cub.2013.09.039.
36. Sparks, E., Wachsman, G., and Benfey, P.N. (2013). Spatiotemporal signalling in plant development. Nat. Rev. Genet. *14*, 631–644.
37. Schlereth, A., Möller, B., Liu, W., Kientz, M., Flipse, J., Rademacher, E.H., Schmid, M., Jürgens, G., and Weijers, D. (2010). MONOPTEROS controls embryonic root initiation by regulating a mobile transcription factor. Nature *464*, 913–916.